



Palladium nanoparticles confined in the nanocages of SBA-16: Enhanced recyclability for the aerobic oxidation of alcohols in water

Zhancheng Ma^a, Hengquan Yang^{a,*}, Yong Qin^b, Yajuan Hao^a, Guang Li^a

^a School of Chemistry and Chemical Engineering, Shanxi University, Taiyuan 030006, China

^b School of Chemistry and Chemical Engineering, Changzhou University, Changzhou 213164, China

ARTICLE INFO

Article history:

Received 16 March 2010

Received in revised form 12 July 2010

Accepted 3 August 2010

Available online 12 August 2010

Keywords:

Mesoporous material

Alcohol oxidation

Palladium nanoparticle

Water

ABSTRACT

Via modification of mesoporous cage-like material SBA-16 followed by adsorption of Pd(OAc)₂ and reduction with NaBH₄, Pd nanoparticles with a uniform size distribution were successfully confined in the nanocages of SBA-16, leading to a new solid catalyst for the aerobic oxidation of alcohols. The solid catalyst was characterized with N₂ sorption, XRD, TEM, FT-IR and XPS. Such a catalyst showed a high activity for the oxidation of benzylic alcohols, 1-phenylethanol and allylic alcohols without the presence of bases under air or O₂ atmosphere in water even at room temperature. The selectivities for the corresponding aldehydes and ketones were more than 99% in all the cases investigated. The developed catalyst could be facilely recovered and reused twelve times without significant decreases in activity and selectivity. Its recyclability was much better than that of the catalyst derived from amorphous silica under the same conditions.

© 2010 Elsevier B.V. All rights reserved.

1. Introduction

The selective oxidation of alcohols to carbonyl compounds is one of the most important transformations in the synthesis of the fine chemicals [1–5]. Currently, of particular interest in this field is the use of molecular oxygen as oxidant because it represents a green process in contrast to the use of toxic and expensive stoichiometric metal oxidants [6–12]. When molecular oxygen is used as oxidant, water may be the most ideal solvent for the industrial applications because it avoids explosions and the hazards associated with the use of oxidisable organic solvents under oxygen pressure [13,14]. In this context, the development of the efficient catalytic systems for the aerobic oxidation of alcohols in water medium is currently an important topic.

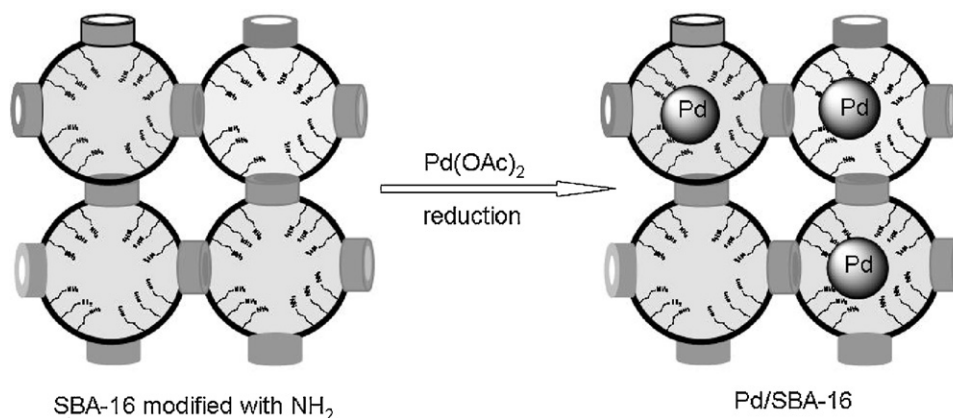
Recently, various supported metal catalysts (Pd, Au, Pt, Ru) were found to be active in the aerobic oxidation of alcohols in water [15–23]. Among these supported catalysts, palladium-based catalysts show promising catalytic performances because they can selectively catalyze the reaction even under the mild (neutral pH) conditions [24–26]. The progress along this line is considerably notable. However, the highly recyclable catalysts that could work in pure water are still rather limited.

One of the key factors that limit the recyclability of the catalysts, is related to the Pd particle sizes. The previous studies showed that

the catalytic activity for the aerobic alcohol oxidation depended on the Pd particle sizes and Pd particles of a few nanometers exhibited the highest activity for the aerobic oxidation of benzyl alcohol [27,9]. However, due to the Ostwald ripening, the palladium nanoparticles of such sizes are prone to growth into the larger particles even Pd black during the catalyst preparation and the followed catalytic reaction. Thus, it is difficult to control the particle sizes in a desired range during the catalyst preparation and maintain the sizes in the sequent catalytic reactions. As reported, the Pd nanoparticles supported on silica evolved into the particles with dozens of nanometers in size after the first reaction cycle [19]. The growth of Pd nanoparticles causes a substantial deactivation of the catalyst.

Among various supports for efficiently preventing the growth of metal nanoparticles, the mesoporous materials are very promising because of their regularly arranged pore structure on a mesoscopic scale. More interestingly, different to the widely used channel-like mesoporous materials MCM-41 and SBA-15, the recently synthesized SBA-16 (cubic, *Im3m*) is one of new ordered mesoporous materials with cage-like structures [28–30]. This mesoporous cage-like material has tunable cage size (4–10 nm) and pore entrance size (generally less than 4 nm). One isolated nanocage is three-dimensionally interconnected by eight neighboring pore entrances, which are more resistant to pore blocking and allow a fast transport of reactants and products. Such isolated nanocages of SBA-16 can not only accommodate metal complexes and metal particles formed *in situ*, but also limit the growth of metal nanoparticles by the spatial restrictions [31–34]. Meanwhile, the smaller pore

* Corresponding author. Tel.: +86 351 7011588; fax: +86 351 7011688.
E-mail address: hqyang@sxu.edu.cn (H. Yang).



Scheme 1. Schematic description for the preparation of the solid catalyst Pd/SBA-16.

entrances may inhibit the motion of metal nanoparticles, thereby preventing the undesired aggregation and agglomeration. Furthermore, SBA-16 has a good stability which is a prerequisite of the applications involving high temperature and the presence of water [35]. However, to our knowledge, the mesoporous cage-like material SBA-16 owning such unique nano-architectures and properties was not explored to support metal particles for the aerobic oxidation of alcohols in water.

In this context, mainly aiming to improve the recyclability of the Pd-supported catalyst for the aerobic oxidation of alcohols in water, we chose the cage-like mesoporous material SBA-16 as a support. Through modification of SBA-16 surface with moderate polarity groups (aminopropyl), sequential adsorption of $\text{Pd}(\text{OAc})_2$ and reduction, Pd particles of a few nanometers were successfully confined inside the nanocages of SBA-16, yielding an active catalyst for the aerobic oxidation of alcohols in water. The recyclability of the catalyst is significantly enhanced, compared with the catalyst derived from amorphous silica.

2. Experimental

2.1. Reagents and materials

Pluronic P123 copolymer ($\text{EO}_{20}\text{PO}_{70}\text{EO}_{20}$), Pluronic copolymer F127 ($\text{EO}_{106}\text{PO}_{70}\text{EO}_{106}$) were purchased from Sigma Company. Tetraethyl orthosilicate and benzyl alcohol were obtained from Shanghai Chemical Reagent Company of Chinese Medicine Group. 3-Aminopropyltriethoxysilane and other alcohols as reactants were purchased from Alfa Aesar. $\text{Pd}(\text{OAc})_2$ was obtained from Hangzhou Kaida and purified before use. Amorphous silica gel with specific surface area of $345\text{ m}^2/\text{g}$ was obtained from Qidao Haiyang Chemical Plant.

Mesoporous cage-like material SBA-16 was synthesized according to the modified method [29]. A mixture of F127 ($\text{EO}_{106}\text{PO}_{70}\text{EO}_{106}$, 7.42 g) and P123 ($\text{EO}_{20}\text{PO}_{70}\text{EO}_{20}$, 1.19 g) were used as the templates. After the mixed templates were completely dissolved in a solution of 300 mL of distilled water and 52.5 g of concentrated hydrochloric acid (36%), and the solution was further stirred at 308 K. After 4 h, 28 mL of tetraethyl orthosilicate was dropwise added to the solution. After stirring for 40 min, the resultant suspension was transferred into autoclaves. The autoclaves were placed under static conditions at 35°C for 24 h. Afterward, the temperature of autoclaves was raised up to 100°C and further kept at this temperature for 32 h. After the hydrothermal treatment, the precipitated solid was isolated by a filtration and dried at 100°C for 24 h, yielding white solid powders. This powder sample was then subjected to a calcination at 550°C for 10 h

and the mesoporous cage-like material SBA-16 was eventually obtained.

2.2. Introduction of Pd nanoparticles into the nanocages of SBA-16

6 g of SBA-16 (evacuated at 125°C for 6 h) was dispersed in 50 mL of dry toluene. Into this system 9.6 mmol of 3-aminopropyltriethoxysilane was added. After stirring for 12 h at 100°C under a N_2 atmosphere, the resulting solid was isolated by a filtration, and repeatedly washed with toluene and then dried under vacuum overnight to give SBA-16 modified with amino groups.

1.2 g of amino-modified SBA-16 was dispersed into 12 mL of toluene containing a given amount of $\text{Pd}(\text{OAc})_2$. After the mixed system was then stirred at room temperature for 6 h, the solid was isolated by a filtration and dried under vacuum. The solid was treated with NaBH_4 in a mixture of toluene and ethanol (20/1, V/V), washed with ethanol and then dried under vacuum, yielding the catalyst Pd/SBA-16.

2.3. Typical procedures for the aerobic oxidation of alcohols

Benzyl alcohol (1 mmol), water (2 mL) and the catalyst Pd/SBA-16 were combined in a dry flask, and the mixture was stirred at given temperature in air or O_2 for a given time. Oxygen gas was introduced into the flask from an O_2 balloon under atmospheric pressure. After the reaction, the liquid was extracted with diethyl ether. The resulting organic layer was dried with Na_2SO_4 and then analyzed with GC to determine the conversion and selectivity.

Recycling test for the aerobic oxidation of alcohol is as follows: for the first reaction cycle, the procedure was the same to above descriptions. After the first reaction cycle, the solid catalyst was recovered by a centrifugation, and extracted repeatedly with ether and ethanol. The recovered catalyst was dried under vacuum and was directly used for the next reaction cycle.

2.4. Characterization and analysis

Small-angle X-ray powder diffraction was performed on Rigaku ($\text{Cu K}\alpha$, 40 kV, 30 mA). N_2 physical adsorption was carried out on micromeritics ASAP2020 volumetric adsorption analyzer (before the measurements, samples were out gassed at 120°C for 6 h). The Brunauer–Emmett–Teller (BET) surface area was evaluated from data in the relative pressure range from 0.05 to 0.20. The total pore volume of each sample was estimated from the amount adsorbed at the highest P/P_0 (above 0.99). Pore diameters were determined from the adsorption branch using Barrett–Joyner–Halenda (BJH)

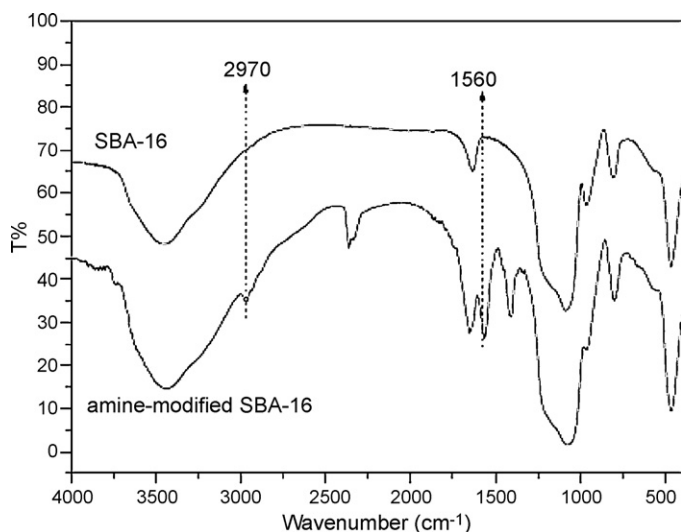


Fig. 1. FT-IR spectra of SBA-16 and amino-modified SBA-16.

method. FT-IR spectra were collected on Thermo-Nicolet-Nexus 470 infrared spectrometer. X-ray photoelectron spectroscopy (XPS) was recorded on Perkin-Elmer 5400 ESCA and C_{1s} line at 284.9 eV was used as the binding energy reference. TEM micrographs were taken using a JEM-2000EX transmission electron microscope at 120 kV.

3. Results and discussion

3.1. Catalyst preparation and characterization

The process for the preparation of the catalyst Pd/SBA-16 is schematically depicted in Scheme 1. In order to introduce Pd precursor into the nanocages of SBA-16, 3-aminopropyltriethoxysilane was employed to modify the surface of SBA-16. Owing to the strong coordination capacity of amino groups, $Pd(OAc)_2$ even with a high loading can be easily adsorbed by SBA-16 modified with amino groups [36]. After a careful reduction of $Pd(OAc)_2$ with $NaBH_4$, Pd(0) was *in situ* yielded and then evolved to nanoclusters. Due to the amino coordination and the spatial restriction by the nanocages of SBA-16, the sizes of Pd(0) clusters were expected to be limited in the range of cage sizes of SBA-16.

The success in grafting amino group on SBA-16 was confirmed with FT-IR spectroscopy. The FT-IR spectra of SBA-16 before and after grafting amino group are shown in Fig. 1. Compared with the FT-IR spectrum of the parent material SBA-16, amino-modified SBA-16 clearly exhibits two new peaks at 2970 and 1560 cm^{-1} , which correspond to the stretching vibrations of the C–H, and the bending vibrations of N–H, respectively. These results indicate that amino groups were successfully grafted on SBA-16. Meanwhile, the intensity of the peak at 960 cm^{-1} (related to the bending vibration of Si–OH on SBA-16) significantly decreased after modification. This also suggests that amino groups were covalently linked with SBA-16 via a silylation reaction.

Amino-modified SBA-16 exhibited a good adsorption capacity towards Pd (OAc)₂ in toluene. 1–10 wt.% Pd with respect to amino-modified SBA-16 could be completely adsorbed by the materials, resulting in a clear solution. Elemental analysis with ICP-AES confirmed that Pd (OAc)₂ was completely introduced onto amino-modified SBA-16. After a treatment with $NaBH_4$, Pd nanoparticles were formed inside the nanocages of SBA-16.

The locations of Pd nanoparticles inside the nanocages of SBA-16 were confirmed by N_2 sorption and TEM. The N_2 sorption isotherms and pore size distribution plots for SBA-16, amino-modified SBA-

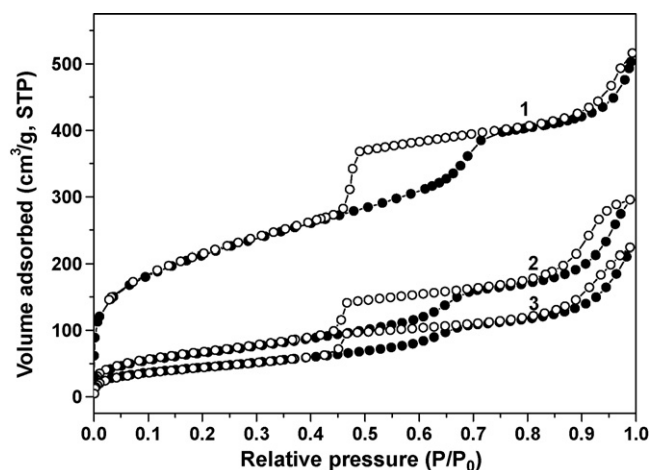


Fig. 2. N_2 sorption isotherms of (1) SBA-16, (2) amino-modified SBA-16 and (3) Pd/SBA-16.

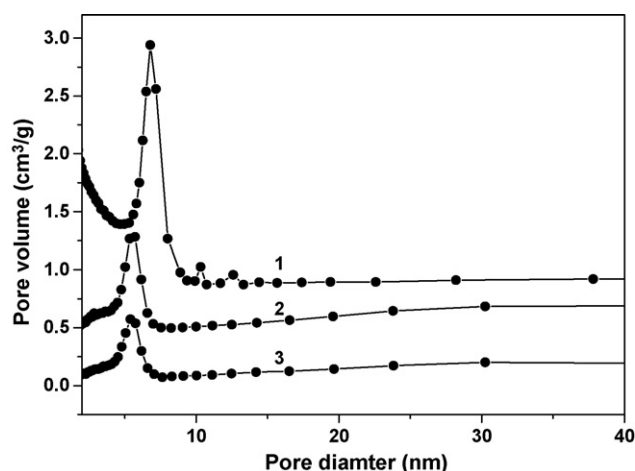


Fig. 3. Pore size distributions of (1) SBA-16, (2) amino-modified SBA-16 and (3) Pd/SBA-16.

16 and Pd/SBA-16, are displayed in Figs. 2 and 3, respectively. The determined textural parameters are listed in Table 1. SBA-16 exhibited a type-IV isotherm pattern with an H2 hysteresis loop in the range of $P/P_0 = 0.4–0.75$, which is characteristic of a mesoporous cage-like structure. Similar to the parent material SBA-16, amino-modified SBA-16 also showed a type-IV isotherm with an H2 hysteresis loop, indicating that SBA-16 after modification still maintained a good mesoporous cage-like structure. It is worth noting that the specific surface area, pore volume and pore size underwent significant decreases after modification (Table 1). Such decreases in these textural parameters are in line with the successful introduction of amino groups onto the internal surface. After adsorption of $Pd(OAc)_2$ and the followed reduction, the specific sur-

Table 1
Textural parameters of SBA-16, SBA-16 modified with NH_2 and Pd/SBA-16.

Samples	Surface area ^a (m^2/g)	Pore volume ^b (cm^3/g)	Cage size ^c (nm)
SBA-16	763	0.80	6.7
Amino-modified SBA-16	240	0.46	5.6
Pd/SBA-16	163	0.33	5.4

^a BET surface area.

^b Single point pore volume calculated at relative pressure P/P_0 of 0.99.

^c BJH method from adsorption branch.

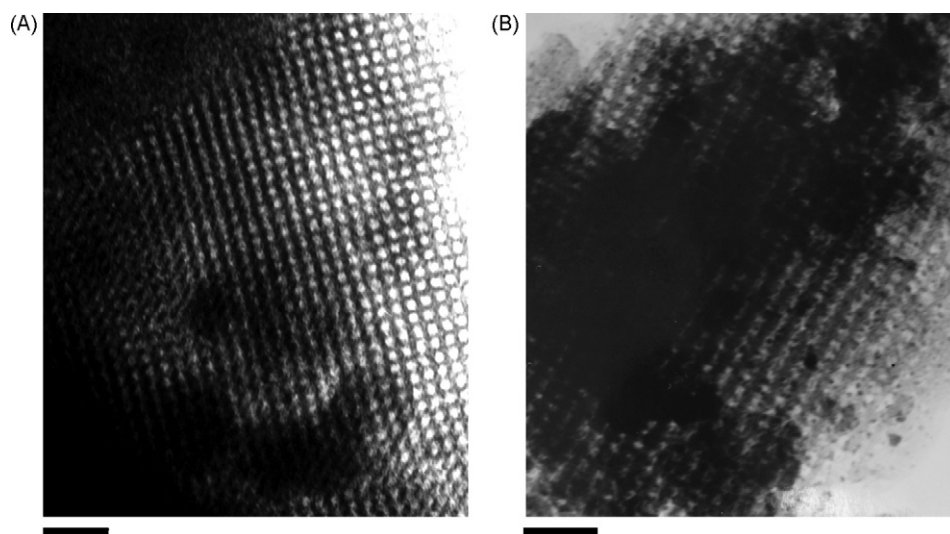


Fig. 4. TEM images for SBA-16 (A) and Pd/SBA-16 (B). The bar is 50 nm.

face area, pore volume and pore size further decreased, suggesting that Pd nanoparticles were located inside the nanocages of SBA-16.

Transmission electron microscopic investigation (TEM) provides a direct evidence for the locations and dimensional information of Pd nanoparticles. The TEM images for SBA-16 and Pd/SBA-16 are presented in Fig. 4A and B, respectively. In Fig. 4A, the (100) projection corresponding to a cubic $Im3m$ structure was clearly observed, XRD pattern of Pd/SBA-16 showed an ordered mesoporous structure similar to the parent SBA-16 (Fig. 5). The TEM and XRD results suggest that the mesoporous cage-like structure of SBA-16 was maintained during the course of preparing the catalyst. After introduction of Pd nanoparticles, the cage-like structure of the catalyst was still observed and fine Pd particles appeared in the nanocages of SBA-16 (Fig. 4B). Interestingly, most of Pd particles with sizes of only a few nanometers were uniformly dispersed in the nanocages of SBA-16.

The Pd(0) on the solid catalyst was further confirmed by XPS. Fig. 6 presents the XPS elemental survey scans of surface elements of the solid catalyst. The peaks corresponding to silicon, oxygen, carbon, nitrogen, palladium elements were clearly observed. Fig. 7 displays Pd binding energy for Pd(OAc)₂ and Pd/SBA-16. Pd(OAc)₂ mainly exhibited two peaks centered at 343.9 and 338.7 eV, which are assigned to Pd 3d_{3/2} and Pd 3d_{5/2} sig-

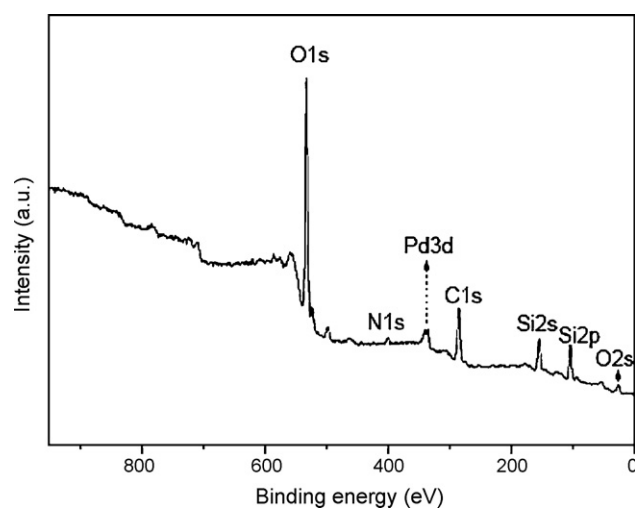


Fig. 6. XPS spectrum for the elemental survey scan of Pd/SBA-16.

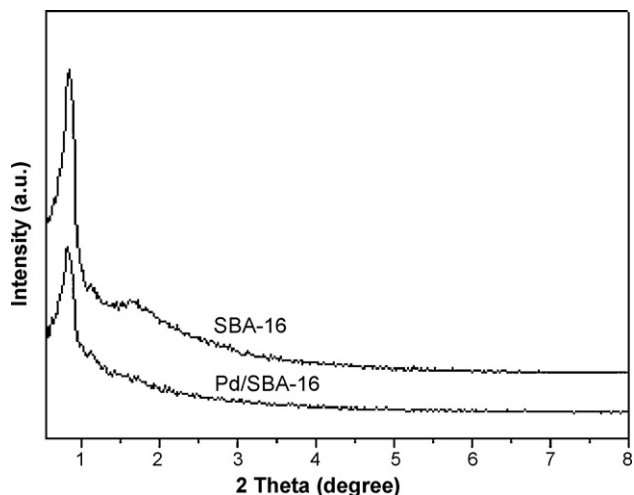


Fig. 5. XRD patterns of SBA-16 and Pd/SBA-16.

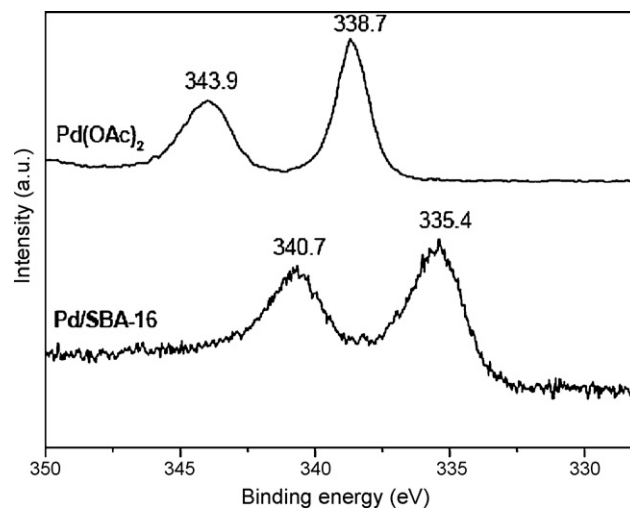


Fig. 7. XPS spectra of Pd binding energy for Pd(OAc)₂ and Pd/SBA-16.

nals, respectively. Compared with Pd(OAc)₂, Pd 3d_{3/2} and Pd 3d_{5/2} peaks for Pd/SBA-16 significantly shift down to 340.7 and 335.4 eV, respectively, indicating that the Pd(II) was transformed to Pd(0) after reduction.

Above characterizations confirm that the prepared catalyst keeps the mesoporous cage-like structure of the parent SBA-16 and the fine Pd(0) nanoparticles were uniformly distributed inside the nanocages of SBA-16.

3.2. The aerobic oxidation of alcohols

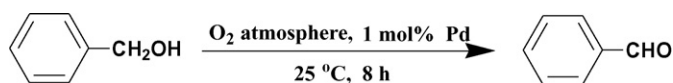
Although several excellent catalysts for the aerobic oxidation of alcohols to the corresponding aldehydes or ketones have been disclosed, most of them required organic solvents, heating and addition of base, which violate the requirements of the “green chemistry”. Water is the most ideal solvent because it is not only a green solvent but also can avoid the hazards associated with the use of oxidisable organic solvents under oxygen pressure. Base-free systems are also highly desired in that the presence of base probably leads to the unwanted by-products. In line with the requirements of “green chemistry”, we chose water as a reaction medium to conduct the aerobic oxidation in the absence of base.

Wang's studies revealed that the catalytic activity of the Pd-based catalyst for the aerobic oxidation of alcohols in organic solvents was dependent on the Pd particle sizes, and Pd particles of 2–4 nm in size were the most active for the aerobic oxidation of benzyl alcohol [27]. Inspired by these findings, we examined the catalytic activities of Pd/SBA-16 with different Pd contents for the aerobic oxidation of alcohols in water because the Pd particle sizes on the support can be associated with the Pd content present on the support. By varying the amount of adsorbed Pd(OAc), five catalysts Pd/SBA-16 with Pd contents from 1 wt.% to 2.5, 4, 5.5, and 10 wt.% were prepared.

The results for the aerobic oxidation of benzyl alcohol in the presence of these five catalysts were presented in Fig. 8. All the tests were conducted in the presence of 1 mol% Pd with respect to alcohols at room temperature under base-free conditions. The catalyst Pd/SBA-16 with a Pd content of 1 wt.% afforded a conversion of 20.5% within 6 h. No by-products such as benzoic acid were detected under the investigated conditions. When the Pd content of the solid catalyst increased up to 2.5 wt.%, the conversion had an apparent increase and a 68.6% conversion was achieved. A further increase in the Pd content up to 4 wt.% led to an increase in the conversion (77.5%). However, when the Pd content continuously increased up to 5.5 wt.%, the conversion began to decrease (a 69.1% conversion). A further increase in the Pd content led to continuous reduces in conversion and a 57.6% conversion was afforded for the catalyst with a Pd content of 10 wt.%. These findings indicate that the catalytic activity of the aerobic oxidation of alcohols is highly dependent on the Pd content present on the solid catalyst. The underlying reason may be related to the Pd particle sizes, as reported by Wang and co-workers [27].

Table 2

The aerobic oxidation of benzyl alcohol over Pd/SBA-16 in different solvents.



Entry	Solvents	Conv. (%)	Select. (%)	Entry	Solvents	Conv. (%)	Select. (%)
1	Acetonitrile	4.8	>99	6	n-Propanol	15.8	>99
2	1,4-Dioxane	7.4	>99	7	Ethanol	20.2	>99
3	DMF	10	>99	8	Methanol	34.0	>99
4	Toluene	15.7	>99	9	H ₂ O	>99	>99
5	n-Butanol	13.7	>99				

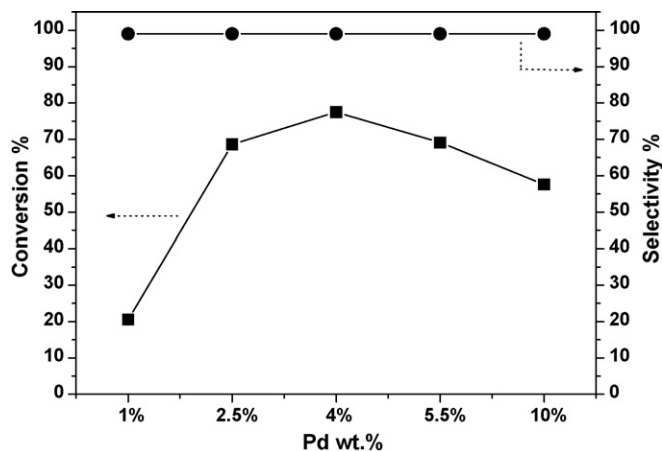
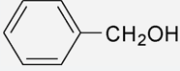
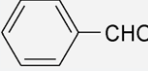
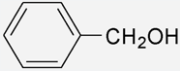
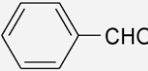
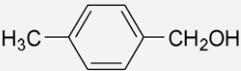
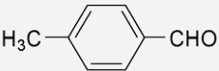
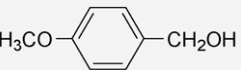
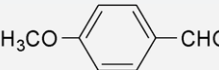
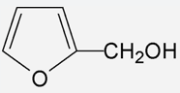
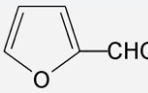


Fig. 8. The aerobic oxidations of benzyl alcohol over the catalysts with variations of the Pd content.

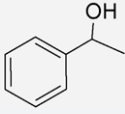
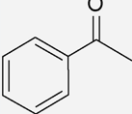
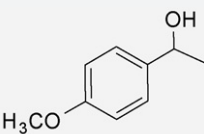
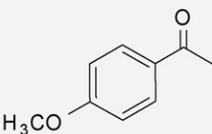
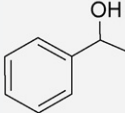
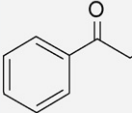
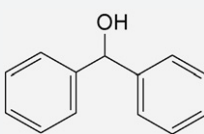
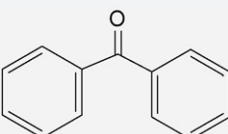
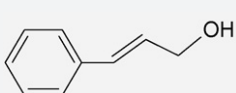
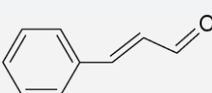
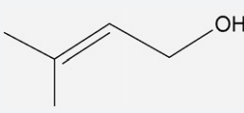
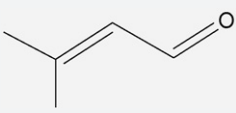
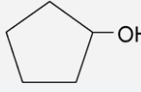
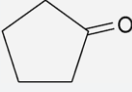
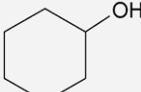
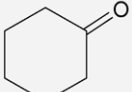
Above examinations revealed that Pd/SBA-16 with a Pd content of 4 wt.% exhibited the highest activity for the aerobic oxidation of benzyl alcohol in water under the base-free conditions. In our previous investigations, it was found that the catalytic reaction occurring in the nanopores had different solvent effects with that in homogeneous solution [32]. In order to test the possibility that Pd/SBA-16 was more active in other reaction media, we examined the activity of the catalyst in a set of solvents under the same conditions. The results are summarized in Table 2. Using acetonitrile, 1,4-dioxane, DMF and toluene as solvents, the conversions of benzyl alcohol were low (less than 16%, Table 2, entries 1–4). When the solvent was changed to alcohols, the conversion was found to increase (Table 2, entries 5–8) and the maximum conversion (34%) was obtained for the case of methanol as solvent. Impressively, using water as the reaction medium led to the fastest conversion of benzyl alcohol. These comparative results show that in the case of our catalyst water is not only a green solvent but also can promote the aerobic oxidation of benzyl alcohol under base-free conditions. This can probably be partially explained that water (with a high polarity) forces the organic substrates to be enriched on the surface (with a moderate polarity) of the solid catalyst and the accessibility of substrates to Pd is thus improved, leading to a high reaction rate.

To further test the performances of the catalyst Pd/SBA-16, the oxidations of other benzylic alcohols with air or O₂ at room temperature was carried out. The results are summarized in Table 3. At Pd loading of 1 mol%, a complete conversion of benzyl alcohol was observed under O₂ atmosphere over 8 h. Under air, although the reaction time needed to be prolonged to 12 h, a complete conversion of benzyl alcohol was still afforded. Whether under O₂ or in air, the selectivity for benzaldehyde exceeded 99%, and no by-product (benzoic acid) was detected within a given time. If the reaction time was prolonged under air or O₂ atmosphere, the by-product benzoic acid (further oxidation of benzaldehyde) was observed. When

Table 3The aerobic oxidation of benzylic alcohols over Pd/SBA-16.^a

Entry	Substrates	Product	Air (12 h)		O ₂ (8 h)	
			Conv. (%)	Select. (%)	Conv. (%)	Select. (%)
1			>99	>99	>99	>99
2 ^b			–	–	>99	>99
3			>99	>99	>99	>99
4			>99	>99	>99	>99
5			–	–	76.3	>99

^a The reaction was carried out in air or O₂ atmosphere in the presence of 1 mol% Pd.^b The reaction was conducted at 50 °C for 4 h.**Table 4**The aerobic oxidation of other alcohols over Pd/SBA-16.^a

Entry	Substrates	Product	Pd (mol%)	Temp. (°C)	Time (h)	Conv. (%)	Select. (%)
1			1.0	50	10	96.9	>99
2			1.0	60	24	87.6	>99
3			1.0	50	10	90.8	>99
4			1.0	90	24	97.8	>99
5			1.0	25	12	>99	>99
6			1.0	50	12	89.5	>99
7			1.0	60	12	16.2	>99
8			2.5	60	12	22.6	>99

^a The reaction was carried out in O₂ atmosphere.

the reaction temperature was raised up to 50 °C, it took only 4 h to complete the reaction (Table 3, entry 2). For CH₃- and CH₃O-substituted benzylic alcohols, over 99% conversions with more than 99% of selectivities were also achieved under O₂ atmosphere over 8 h (Table 3, entries 3 and 4). Under air, it also took a longer time (12 h) to obtain complete conversions. For heterocyclic alcohols, the catalyst Pd/SBA-16 showed a moderate activity with excellent selectivity (Table 3, entry 5).

The aerobic oxidation of other alcohols in water was investigated to further examine the application range of the catalyst Pd/SBA-16. Representative results are summarized in Table 4. For 1-phenylethanol, at Pd loading of 1 mol% the catalyst Pd/SBA-16 gave a 96.9% conversion within 10 h (Table 4, entry 1). The selectivity for acetophenone was observed to be more than 99%. For methoxy-substituted 1-phenylethanol, it needed 24 h to achieve a good conversion (Table 4, entry 2). Compared with 1-phenylethanol, the electron-rich methoxy-substituted 1-phenylethanol was less reactive. The selectivity was still up to 99%. For 1-phenylpropanol, a 90.8% conversion with 99% selectivity was obtained within 10 h (Table 4, entry 3). A 97.8% conversion of diphenyl methanol could be achieved over Pd/SBA-16 although it required a relatively higher temperature and a longer reaction time (Table 4, entry 4). Pd/SBA-16 also showed high activity for allylic alcohols (Table 4, entries 5 and 6). Cinnamyl alcohol was completely converted to cinnamaldehyde at room temperature within 12 h. For 3-methyl-2-butan-1-ol, an 89.5% conversion was obtained at 50 °C over 12 h. The selectivity for α , β -unsaturated aldehydes was more than 99% for the two cases investigated. For the secondary cyclic alcohols, Pd/SBA-16 shows a relatively low activity. A 16.2% conversion of cyclopentanol and a 22.6% conversion of cyclohexanol were afforded (Table 4, entries 7 and 8). The above investigations showed that the developed catalyst Pd/SBA-16 had a moderate substrate scope in water under base-free conditions.

Further experiments were performed to verify the recyclability of the developed solid catalyst. The consecutive oxidations of benzyl alcohol in O₂ atmosphere were also carried out at 50 °C under base-free conditions using water as solvent. The results are reflected in Fig. 9. At Pd loading of 1 mol%, Pd/SBA-16 afforded a complete conversion under O₂ atmosphere over 4 h. After the first reaction cycle, the resulting product was extracted with ether three times. The catalyst was recovered by a centrifugation and dried

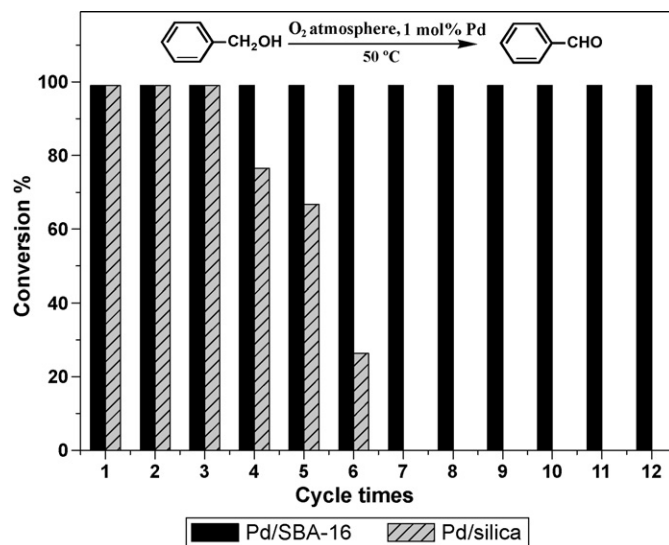


Fig. 9. The recyclability tests of Pd/SBA-16 and Pd/silica for the aerobic oxidation of benzyl alcohol.

for the next cycles. For the second reaction cycle, the fresh benzyl alcohol was added and other conditions were the same as the first reaction cycle. A 99% conversion was still obtained over 4 h. From the third to 12th reaction, 99% conversions could be achieved. The selectivity for benzaldehyde was kept at >99% throughout the 12 reaction cycles. Such a recyclability of Pd/SBA-16 represents one of the best results for the alcohol oxidation in water.

The recyclability of Pd/SBA-16 is impressive in view of water as a solvent. In order to further understand the high recyclability, Pd nanoparticles were supported on amorphous silica through the same procedures, resulting in a catalyst Pd/silica (the Pd loading was the same to the Pd/SBA-16). Comparative tests for the recyclability were conducted under the same conditions. The results for Pd/silica are also included in Fig. 9. From the first to the third reaction cycle, the catalyst Pd/silica could afford a complete conversion of benzyl alcohol and the selectivity also exceeded 99%. But from the fourth reaction cycle, the conversion began to decrease and a

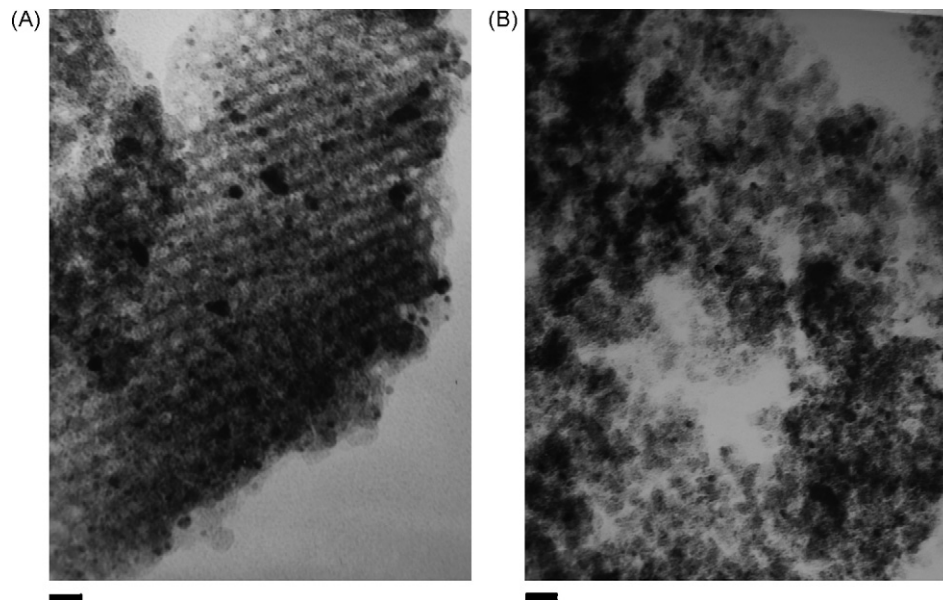


Fig. 10. TEM images for (A) Pd/SBA-16 used four times and (B) Pd/silica used four times. The bar is 20 nm.

conversion of only 76.5% was obtained. For the followed fifth and sixth reaction cycles, the conversions further decreased to 66.7% and 26.4%, respectively. Obviously, the recyclability of Pd/SBA-16 was much better than that of Pd/silica.

The significantly enhanced recyclability of the catalyst may be partially attributable to the unique structure of SBA-16. To confirm the role of the pore structure, TEM was employed to characterize Pd/SBA-16 used four times and Pd/silica used four times. Their TEM images are presented in Fig. 10A and B, respectively. For the catalyst Pd/SBA-16 used four times, the cage-like structure of parent material SBA-16 could be still observed although the structure was subjected to collapse to some extent. It is worthwhile to note that most of fine Pd particles with sizes of less than 5 nm were dispersed in the cages of SBA-16 although a small portion of larger Pd particles are located on the external surface of SBA-16. While for the catalyst Pd/silica after being used four times, it was observed that Pd particles were relatively larger and not uniform in size. Additionally, the structure of the parent silica underwent a severe collapse. The size differences of Pd particles between Pd/SBA-16 and Pd/silica partially accounted for their differences in the activities of the recovered catalysts.

The smaller Pd particles with a relatively uniform distribution in size may be attributed to the mesoporous cage-like structure of SBA-16. Due to the high surface energy, the unstable nanoclusters are prone to growing into larger particles through aggregation and agglomeration. Owing to the spatial restriction of the isolated nanocages and smaller pore entrances of SBA-16, the aggregation and agglomeration of Pd nanoclusters were efficiently prevented. However, for the Pd/Silica, it was unable to prevent the growth of Pd nanoparticles because of lacking the ordered cage-like pores. Additionally, a low stability probably led to the structure collapse of silica and a portion of Pd particles were thus buried.

4. Conclusion

By confining Pd nanoparticles in the nanocages of the modified SBA-16, a new solid catalyst for the aerobic oxidations of alcohol was prepared. The catalyst showed high activity for the oxidation of benzylic alcohols, 1-phenylethanol and allylic alcohols under air or O₂ atmosphere in water even at room temperature. The selectivities for the corresponding aldehydes and ketones were more than 99% in all the cases investigated. The catalyst can be facilely recovered and reused twelve times without the changes in the conversion and selectivity, representing the most durable solid catalysts for the alcohol oxidation in water. Its recyclability was much better than that of the catalyst derived from amorphous silica under the same conditions. The significantly enhanced recyclability may be attributed to the high stability and the isolated nanocages of SBA-16 which could efficiently prevent the growth of Pd nanoparticles during the catalytic reaction.

Acknowledgments

We acknowledge New Teacher Foundation from Education Ministry of China (200801081035), the Natural Science Foundation of China (20903064), Shanxi Natural Science Foundation for Youths (2009021009), Shanxi University Innovative Experimental Project for Undergraduates and Jiangsu Key lab for fine petrochemistry for financial supports (KF0802).

References

- [1] T. Mallat, A. Baiker, *Chem. Rev.* 104 (2004) 3037.
- [2] G.J. Brink, I.W.C.E. Arends, R.A. Sheldon, *Science* 287 (2000) 1636.
- [3] M.S. Sigman, D.R. Jensen, *Acc. Chem. Res.* 39 (2006) 221.
- [4] S.S. Stahl, *Angew. Chem. Int. Ed.* 43 (2004) 3400.
- [5] T. Matsumoto, M. Ueno, N.W. Wang, S. Kobayashi, *Chem. Asian J.* 3 (2008) 196.
- [6] Y.H. Ng, S. Ikeda, T. Harada, Y. Morita, M. Matsumura, *Chem. Commun.* (2008) 3181.
- [7] Y.M.A. Yamada, T. Arakawa, H. Hocke, Y. Uozumi, *Angew. Chem. Int. Ed.* 46 (2007) 704.
- [8] A. Abad, A. Corma, H. García, *Chem. Eur. J.* 14 (2008) 212.
- [9] J. Chen, Q.H. Zhang, Y. Wang, H.L. Wan, *Adv. Synth. Catal.* 350 (2008) 453.
- [10] B.A. Steinhoff, A.E. King, S.S. Stahl, *J. Org. Chem.* 71 (2006) 1861.
- [11] B. Karimi, A. Biglari, J.H. Clark, V. Budarin, *Angew. Chem. Int. Ed.* 46 (2007) 7210.
- [12] I.W.C.E. Arends, G.J. Brink, R.A. Sheldon, *J. Mol. Catal. A: Chem.* 251 (2006) 246.
- [13] A. Biffis, L. Minati, *J. Catal.* 236 (2005) 405.
- [14] W. Hou, N.A. Dehm, R.W.J. Scott, *J. Catal.* 253 (2008) 22.
- [15] T. Wang, H. Shou, Y. Kou, H.C. Liu, *Green Chem.* 11 (2009) 562.
- [16] J.H. Liu, F. Wang, K.P. Sun, X.L. Xu, *Adv. Synth. Catal.* 349 (2007) 2439.
- [17] R.L. Oliveira, P.K. Kiyohara, L.M. Rossi, *Green Chem.* 12 (2010) 144.
- [18] H.R. Li, B.T. Guan, W.J. Wang, D. Xing, Z. Fang, X.B. Wan, L.P. Yang, Z.J. Shi, *Tetrahedron* 63 (2007) 8430.
- [19] B. Karimi, A. Zamani, S. Abedi, J.H. Clark, *Green Chem.* 11 (2009) 109.
- [20] J. Yang, Y.J. Guan, T. Verhoeven, R. Van Santen, C. Li, E.J.M. Hensen, *Green Chem.* 11 (2009) 322.
- [21] P. Paraskevopoulou, N. Psaroudakis, S. Koinis, P. Stavropoulos, K. Mertis, *J. Mol. Catal. A: Chem.* 240 (2005) 27.
- [22] Y. Uozumi, R. Nakao, *Angew. Chem. Int. Ed.* 42 (2003) 194.
- [23] Y.M.A. Yamada, Y. Uozumi, *Org. Lett.* 8 (2006) 1375.
- [24] H. Wang, S.X. Deng, Z.R. Shen, J.G. Wang, D.T. Ding, T.H. Chen, *Green Chem.* 11 (2009) 1499.
- [25] Z.S. Hou, N. Theyssen, A. Brinkmann, K.V. Klementiev, W. Grünert, M. Bühl, W. Schmidt, B. Spliethoff, B. Tesche, C. Weidenthaler, W. Leitner, *J. Catal.* 258 (2008) 315.
- [26] K.M. Gligorich, M.S. Sigman, *Chem. Commun.* (2009) 3854.
- [27] F. Li, Q.H. Zhang, Y. Wang, *Appl. Catal. A: Gen.* 334 (2008) 217.
- [28] H. Skaff, T. Emrick, *Chem. Commun.* (2003) 52.
- [29] T.W. Kim, R. Ryoo, M. Kruk, K.P. Gierszal, M. Jaroniec, S. Kamiya, O. Terasaki, *J. Phys. Chem. B* 108 (2004) 11480.
- [30] O.C. Gobin, Y. Wan, D.Y. Zhao, F. Kleitz, S. Kaliaguine, *J. Phys. Chem. C* 111 (2007) 3053.
- [31] H.Q. Yang, J. Li, J. Yang, Z.M. Liu, Q.H. Yang, C. Li, *Chem. Commun.* (2007) 1086.
- [32] H.Q. Yang, X.J. Han, G. Li, Y.W. Wang, *Green Chem.* 11 (2009) 1184.
- [33] H.Q. Yang, L. Zhang, L. Zhong, Q.H. Yang, *Can Li, Angew. Chem. Int. Ed.* 46 (2007) 6861.
- [34] H.Q. Yang, L. Zhang, P. Wang, Q.H. Yang, *Can Li, Green Chem.* 11 (2009) 257.
- [35] M. Kruk, C.M. Hui, *J. Am. Chem. Soc.* 130 (2008) 1528.
- [36] R. Xing, Y.M. Liu, H.H. Wu, X.H. Li, M.Y. He, P. Wu, *Chem. Commun.* (2008) 6297.